IET Research Journals

Submission Template for IET Research Journal Papers

IET Journals
The Institution of Engineering and Technology

ISSN 1751-8644
doi: 0000000000
www.ietdl.org

Nonlinear-disturbance-observer-enhanced MPC for motion control systems with multiple disturbances

Yunda Yan[1], *Jun Yang*[1], *Zhenxing Sun*[2], *Shihua Li*[1*], *Haoyong Yu*[3]

[1] *Key Laboratory of Measurement and Control of Complex Systems of Engineering, Ministry of Education, School of Automation, Southeast University, Nanjing, Jiangsu 210096, People's Republic of China*
[2] *College of Electrical Engineering and Control Science, Nanjing Tech University, Nanjing, Jiangsu 211816, People's Republic of China*
[3] *Department of Biomedical Engineering, Faculty of Engineering, National University of Singapore, Singapore 117576, Singapore*
* *E-mail: lsh@seu.edu.cn*

Abstract: This paper addresses the optimized tracking problem for motion control systems with multiple disturbances by a nonlinear-disturbance-observer-enhanced continuous-time model predictive control (MPC) method. The core is to predict the future tracking error and desired control input (including the lumped effects of disturbances/uncertainties) in the receding-horizon by a higher-order sliding mode disturbance observer, which is designed based upon a rough nominal system. Different from direct compensation approach in most existing composite MPC methods, disturbance estimates are taken full advantage in the optimization. The explicit relationship between asymptotic stability and weights in the performance index is provided. Simulations on position control of robot arm system and experiments on speed regulation of permanent magnet synchronous motor (PMSM) servo system are both presented to demonstrate the workability.

1 Introduction

Model predictive control (MPC) method, as one of few suitable methods to deal with optimization, constraints and multivariable plants, has been receiving a great deal of attention in engineerings, particularly in process control industries, e.g., oil refining, pulp and paper manufacturing and chemical processing [1–3]. For large-scale process networks, e.g., reactor-separator, distributed MPC methods also manage to position themselves due to advantages in decomposition and computational efficiency [4–6]. As its name suggested, the nominal model plays a fundamental role in the philosophy of MPC methods, especially in the phase of model prediction. Consequently, in practical applications, efforts on plant modeling have to be paid for high-precision tracking performance of MPC methods. For complex nonlinear models, multiple linear ones can be used to capture the essence of the nonlinear part by fuzzy [7] and adaptive approaches [8]. Apart from modeling errors, external disturbances also inevitably bring barriers to higher-precision prediction, and eventually generate undesirable influences on the closed-loop control performance[9–11]. Therefore, how to attenuate the adverse effects caused by disturbances and uncertainties is always important and should be taken into account by most researchers. The mainstream MPC approaches to handle this problem can be roughly classified into the following two categories.

The first category approaches are referred to as the integral MPC (I-MPC) method (see [12] for theoretical guidance and [13–15] for application cases). I-MPC method applies a performance index which consists of the tracking error and the control difference/rate (i.e., $u(k) - u(k-1)$ in discrete-time domain or $\dot{u}(t)$ in continuous-time domain). The optimal control difference/rate is obtained by directly minimizing the performance index. Since an integral action is naturally embedded in the closed-loop system from the designed control difference/rate to the control input, I-MPC method is able to remove the offset caused by constant disturbances. However, for the system subject to non-constant disturbances, the steady-state tracking error is generally inevitable. In addition, these approaches which regulate the steady-state error via integral compensating action will also cause side effects on other dynamic control performance, e.g., settling time and overshoot [16], which are also important in motion control systems.

The second category focuses on utilizing the disturbance observer to improve the robustness and disturbance rejection performance of MPC methods. Disturbance observer is a kind of special soft sensors to estimate the lumped effect of system uncertainties and external disturbances (see [17–20], and the references therein). These approaches can also be sketchily classified into the following two branches:

i) *Direct Disturbance Compensation Approaches:* In this branch, disturbance observer totally acts as a "patch", since the final composite control law is designed by simply and directly combining the disturbance estimates into the optimal MPC law designed based upon the nominal plant [7, 21–23]. Disturbance estimates are employed to cancel the adverse effect caused by uncertainties and disturbances. Due to the additional disturbance compensation, the composite control law is actually not optimal any more and is also possible to break the system constraints obtained by the original MPC design, especially when large disturbances appear.

ii) *Prediction-precision Enhanced Approaches:* This branch utilizes disturbance estimates to improve the precision of the prediction model [10, 11, 24–26]. Based on the corrected prediction model, the offset-free optimal tracking is obtained by solving the performance index. Linear and nonlinear discrete-time MPC methods with constant disturbances are proposed in [10] and [11], respectively whilst linear discrete-time MPC method with disturbances generated by a linear exosystem is proposed in [24]. In [25], continuous-time nonlinear generalized predictive control (NGPC) method with disturbance observer designed based on constant disturbance model is proposed for nonlinear systems. However, the control input weighting is not explicitly taken into account in the performance index, i.e., $J = \frac{1}{2}\int_0^T (y(t+\tau) - y_d(t+\tau))^2 d\tau$ in [25], which spontaneously makes the controller lose the freedom of penalizing the control energy. A new performance index integrating control input weighting is developed for MPC method in [26]. However, the

steady-state tracking error always exists, even if the plant is free of disturbances or uncertainties.

In addition, most of the above-mentioned disturbance observer based MPC approaches mainly focus on removing the offset caused by constant disturbances. One possible reason is that the dynamics of process control industries are sufficiently slow, as compared with the computation rates of processors. In the presence of time-varying disturbances, those approaches could only obtain practical stability but fail to achieve asymptotic stability, leading to the negligent presence of MPC methods in motion control systems. In a motion control system, whose dynamics is much faster than that of the process control one, the model of lumped disturbances cannot be simply regarded as unknown constant in high-performance applications. As reported in [27], various kinds of disturbances exist in motion control systems. For example, the effects of non-ideal actuators and sensors in a permanent magnet synchronous motor (PMSM) servo system can be regarded as periodic disturbances on the control input (voltage) whilst the effects of external load/friction torques can be as polynomial ones. The existing multiple kinds of disturbances will largely restrain the applicability of MPC methods in motion control systems to achieve high-precision tracking.

Motivated by above-mentioned challenges, an enhanced continuous-time MPC approach is proposed to achieve optimized offset-free tracking for motion control systems with multiple kinds of disturbances. The design philosophy of the proposed method is explicitly demonstrated in the following two phases. First, a higher-order sliding mode disturbance observer [28] is adopted to estimate both states and disturbances of the tracking error system, and thereafter these estimates are utilized to predict the future error in the receding-horizon time interval by virtue of Taylor series expansion. Second, a modified performance index which consists of both the tracking error and the control input is proposed, and then, receding-horizon optimization based on the new performance index is processed to derive the final control law. Comparing to the previous related MPC results concerning on the disturbance attenuation, the main contributions of this paper are summarized by the following two aspects:

i) *Integral Control Optimization:* Inspired by the target control inputs in offset-free MPC methods [10, 11, 24], the control input weighting is explicitly integrated in the performance index of continuous-time NGPC method, which provides additional freedom to penalize the control energy and admits the integral control optimization of the closed-loop system. Besides, as a further result of [29], the effects of control input weighting on the closed-loop stability is explicitly analyzed.
ii) *Multiple Disturbance Attenuation:* Unlike the conventional linear disturbance observer based MPC methods [10, 11, 21–26], the proposed approach does not require an exact disturbance model to achieve a high-precision estimation due to the robustness property of sliding model method. Offset-free optimized tracking is then guaranteed for motion control systems with multiple kinds of disturbances, where only bounded condition is required on disturbances.

The remainder of this paper is organized as follows. Section 2 describes the design of the proposed enhanced MPC method, including the modified performance index, the prediction of both tracking error and desired control input with corrections by higher-order sliding mode disturbance observer and the receding-horizon optimization. Stability analysis of the closed-loop system is also provided in Section 2, whose proof is collected in Appendix. Simulation studies on position control of robot arm system is presented at the end of Section 2 whilst various comparative experimental studies to other effective MPC methods [12, 26] on a PMSM servo system is given in Section 3. Section 4 concludes this paper.

Notation: Throughout the paper, symbols $\mathbb{R}$, $\mathbb{N}$ and $\mathbb{N}_+$ denote the real number set, the natural number set and the positive integer set, respectively. $\mathbb{N}_{i:j}$ is defined as $\mathbb{N}_{i:j} \triangleq \{i, i+1, \cdots, j\}$ for $i, j \in \mathbb{N}$ and $i \leq j$. $\forall M \geq 0 \in \mathbb{R}_{n\times n}$ and $x \in \mathbb{R}_{n\times 1}$, let $\|x\|_M^2 \triangleq x^\top Mx$ and $\|x\|^2 \triangleq x^\top x$. For any smooth enough function $f(t)$, symbol $f^{(i)}(t)$ denotes the i-th order derivative of $f(t)$ with respect to variable t.

2 Main Results

In this paper, a class of generalized motion control systems with external disturbances is considered and depicted by

$$y^{(n)}(t) = f\left(y(t), y^{(1)}(t), \cdots, y^{(n-1)}(t), d(t), t\right) + b(t)u(t) \tag{1}$$

where $y(t) \in \mathbb{R}$, $u(t) \in \mathbb{R}$, and $d(t) \in \mathbb{R}$ are the controlled output, the control input, and the external disturbance, respectively; $y^{(i)}(t)$ is the i-th derivative of $y(t)$ with respect to t; and $b(t)$ is the control gain which satisfies $\underline{b} \leq b(t) \leq \bar{b}$, $\underline{b}$ and $\bar{b}$ are both positive constants. The objective of this paper is to solve an optimized tracking problem, i.e., design a controller to render the output of the disturbed system (1) asymptotically track a reference signal $y_r(t)$ in terms of a performance index, which will be given in the next subsection.

For the sake of simplicity, the following transformation (2) is firstly defined by

$$e(t) \triangleq y_r(t) - y(t),\ x_i(t) \triangleq e^{(i-1)}(t),\ i \in \mathbb{N}_+ \tag{2}$$

where $y_r(t)$ is assumed to be piecewise continuous, n-th time differentiable and bounded. Note that $x_1(t) = e(t)$. The tracking error dynamics is then obtained as

$$\begin{aligned} \dot{x}_i(t) &= x_{i+1}(t),\ i \in \mathbb{N}_{1:n-1} \\ \dot{x}_{n+j}(t) &= -b_0 u^{(j)} + z_{j+1}^n(t) + z_{j+1}(t),\ j \in \mathbb{N} \end{aligned} \tag{3}$$

where $w_n(t) \triangleq y_r^{(n)}(t), w(t) \triangleq (b_0/b(t) - 1)\, y^{(n)}(t) - b_0/b(t) f(\cdot)$, $z_{j+1}^n(t) \triangleq w_n^{(j)}(t)$, $z_{j+1}(t) \triangleq w^{(j)}(t)$ and b_0 is the nominal value of $b(t)$.

Remark 1. *The function $w_n(t)$ contains the known reference signal whilst the function $w(t)$ represents the lumped effect of the unknown disturbances and uncertainties.*

Remark 2. *The considered system (1) is a more generalized model developed from the practical motion control systems. It is worth pointing out here that the practical motion systems, from a simple one- or two-order system [17] to a complicated robot system [30–32], can be all regarded as one single system (1) or several cascaded systems generated by (1). And hence, the design of the MPC method for system (1) to achieve high-performance tracking is fundamental and significant for motion control systems.*

2.1 Modified Performance Index

Inspired by the target control inputs in offset-free MPC methods [10, 11, 24], a modified and generalized performance index with explicit control input weighting is introduced for continuous-time NGPC method, as follows

$$\begin{aligned} J(t) = \frac{1}{2}\int_0^T \Big(&\|y_r(t+\tau) - y(t+\tau)\|_Q^2 \\ &+ \|u_r(t+\tau) - u(t+\tau)\|_R^2 \Big) d\tau \end{aligned} \tag{4}$$

where $T > 0$ is the predictive period; $u_r(t)$ is the desired steady-state control input, denoted as $u_r(t) \triangleq (w_n(t) + w(t))/b_0$; and $Q > 0$ is the weight on the tracking error and $R \geqslant 0$ is the weight on the control input.

Remark 3. *In the conventional NGPC method [25, 29, 33, 34], only the tracking error is considered in the performance index and*

the control energy only can be implicitly penalized by increasing the predictive period. Besides, the control input weighting approach adopted here is different from that in [26] (i.e., $1/2\int_0^T \|u(t+\tau)\|_R^2 d\tau$). Since each part in the performance index tends to zero in the process of optimization, in general, zero control input and zero tracking error are contradictory, especially in the presence of disturbances/uncertainties. This implies that the control input weighting in [26] will usually cause offset tracking error in the presence of non-vanishing disturbances, which will be demonstrated by the later PMSM experimental case studies.

2.2 Disturbance Correction Based Prediction

The future tracking error $e(t+\tau)$ within the predictive period (i.e., $0 \le \tau \le T$) is predicted using Taylor series expansion and given by

$$\begin{aligned} e(t+\tau)\big|_{(2)} \approx\ & e(t) + \tau e^{(1)}(t) + \cdots + \frac{\tau^{n-1}}{(n-1)!}e^{(n-1)}(t) \\ & + \frac{\tau^n}{n!}e^{(n)}(t) + \cdots + \frac{\tau^{n+r}}{(n+r)!}e^{(n+r)}(t) \\ =\ & x_1(t) + \tau x_2(t) + \cdots + \frac{\tau^{n-1}}{(n-1)!}x_n(t) \\ & + \frac{\tau^n}{n!}x_{n+1}(t) + \cdots + \frac{\tau^{n+r}}{(n+r)!}x_{n+1+r}(t) \end{aligned} \tag{5}$$

where $r \in \mathbb{N}$ is named as the control order (detailedly defined in [29]).

For briefness, estimates of the variables are denoted by the hatted symbol $\hat{(\cdot)}$ whilst predictions of the variables within a receding horizon time interval are denoted by the barred symbol $\bar{(\cdot)}$. To this end, by utilizing estimates raised by the disturbance observer, i.e., $\hat{x}_i(t),\ i \in \mathbb{N}_{2:n+1+r}$, the predicted tracking error is presented as

$$\begin{aligned} \bar{e}(t+\tau) =\ & x_1(t) + \tau\hat{x}_2(t) + \cdots + \frac{\tau^{n-1}}{(n-1)!}\hat{x}_n(t) \\ & + \frac{\tau^n}{n!}\hat{x}_{n+1}(t) + \cdots + \frac{\tau^{n+r}}{(n+r)!}\hat{x}_{n+1+r}(t). \end{aligned} \tag{6}$$

Letting the control sequence as

$$\mathcal{U}(t) \triangleq [\ u(t) \quad u^{(1)}(t) \quad \cdots \quad u^{(r)}(t)\ ]^\top,$$

the predicted tracking error $\bar{e}(t+\tau)$ is then expressed by the following compact form

$$\bar{e}(t+\tau)\big|_{(3)} = [\ \bar{\mathcal{T}}(\tau) \quad \tilde{\mathcal{T}}(\tau)\ ] \begin{bmatrix} \bar{\mathcal{E}}(t) \\ \tilde{\mathcal{E}}(t) \end{bmatrix} \tag{7}$$

where

$$\begin{aligned} \bar{\mathcal{T}}(\tau) &\triangleq [\ 1 \quad \tau \quad \cdots \quad \tfrac{\tau^{n-1}}{(n-1)!}\ ] \\ \tilde{\mathcal{T}}(\tau) &\triangleq [\ \tfrac{\tau^n}{n!} \quad \tfrac{\tau^{n+1}}{(n+1)!} \quad \cdots \quad \tfrac{\tau^{n+r}}{(n+r)!}\ ] \\ \bar{\mathcal{E}}(t) &\triangleq [\ x_1(t) \quad \hat{x}_2(t) \quad \cdots \quad \hat{x}_n(t)\ ]^\top \\ \tilde{\mathcal{E}}(t) &\triangleq [\ \hat{x}_{n+1}(t) \quad \hat{x}_{n+2}(t) \quad \cdots \quad \hat{x}_{n+1+r}(t)\ ]^\top \\ &= -b_0\mathcal{U}(t) + \mathcal{W}_n(t) + \mathcal{W}(t) \\ \mathcal{W}_n(t) &\triangleq [\ z_1^n(t) \quad z_2^n(t) \quad \cdots \quad z_{r+1}^n(t)\ ]^\top \\ \mathcal{W}(t) &\triangleq [\ \hat{z}_1(t) \quad \hat{z}_2(t) \quad \cdots \quad \hat{z}_{r+1}(t)\ ]^\top. \end{aligned}$$

It is worth noting that the vector $\mathcal{W}(t)$ is a correction for the conventional prediction based on Taylor series expansion due to the existing disturbances and uncertainties. Similarly, the future control input and the desired control input are written as

$$\bar{u}(t+\tau) = \hat{\mathcal{T}}(\tau)\mathcal{U}(t) \tag{8}$$

$$\bar{u}_r(t+\tau) = \frac{1}{b_0}\hat{\mathcal{T}}(\tau)\left(\mathcal{W}_n(t) + \mathcal{W}(t)\right) \tag{9}$$

where $\hat{\mathcal{T}}(\tau) \triangleq [\ 1 \quad \tau \quad \cdots \quad \frac{\tau^r}{r!}\ ]$.

2.3 Receding-Horizon Optimization

With (7), (8) and (9) in mind, the performance index (4) is predicted as

$$\begin{aligned} \bar{J}(t) =\ & \frac{1}{2}\int_0^T \Big(Q\bar{e}(t+\tau)^\top \bar{e}(t+\tau) \\ & + R\left(\bar{u}(t+\tau) - \bar{u}_r(t+\tau)\right)^\top \left(\bar{u}(t+\tau) - \bar{u}_r(t+\tau)\right)\Big) d\tau \\ =\ & \frac{1}{2}Q\bar{\mathcal{E}}^\top\mathcal{T}_1\bar{\mathcal{E}} - b_0Q\bar{\mathcal{E}}^\top\mathcal{T}_2\left(\mathcal{U} - \frac{1}{b_0}(\mathcal{W}_n + \mathcal{W})\right) \\ & + \frac{1}{2}\left(\mathcal{U} - \frac{1}{b_0}(\mathcal{W}_n + \mathcal{W})\right)^\top \left(b_0^2Q\mathcal{T}_3 + R\mathcal{T}_4\right) \\ & \times \left(\mathcal{U} - \frac{1}{b_0}(\mathcal{W}_n + \mathcal{W})\right) \end{aligned} \tag{10}$$

where $\mathcal{T}_1 \triangleq \int_0^T \bar{\mathcal{T}}^\top\bar{\mathcal{T}}d\tau$, $\mathcal{T}_2 \triangleq \int_0^T \bar{\mathcal{T}}^\top\tilde{\mathcal{T}}d\tau$, $\mathcal{T}_3 \triangleq \int_0^T \tilde{\mathcal{T}}^\top\tilde{\mathcal{T}}d\tau$ and $\mathcal{T}_4 \triangleq \int_0^T \hat{\mathcal{T}}^\top\hat{\mathcal{T}}d\tau$.

Taking partial derivative of $\bar{J}$ in (10) with respect to $\mathcal{U}$ gives $\partial\bar{J}/\partial\mathcal{U} = -b_0Q\mathcal{T}_2^\top\bar{\mathcal{E}} + \left(b_0^2Q\mathcal{T}_3 + R\mathcal{T}_4\right)(\mathcal{U} - (\mathcal{W}_n + \mathcal{W})/b_0)$. Note that the matrix $b_0^2Q\mathcal{T}_3 + R\mathcal{T}_4$ is positive definite. Letting $\partial\bar{J}/\partial\mathcal{U} = 0$ and $\partial^2\bar{J}/\partial\mathcal{U}^2 > 0$, the optimized control sequence $\mathcal{U}^*(t)$ is obtained and given by

$$\mathcal{U}^*(t) = \frac{1}{b_0}\left(\left(\mathcal{T}_3 + \frac{1}{b_0^2}\frac{R}{Q}\mathcal{T}_4\right)^{-1}\mathcal{T}_2^\top\bar{\mathcal{E}} + \mathcal{W}_n + \mathcal{W}\right). \tag{11}$$

Taking the first row of the control sequence (11), the implementable MPC law is given by

$$\begin{aligned} u^*(t) = \frac{1}{b_0}\Big(& k_1x_1(t) + k_2\hat{x}_2(t) + \cdots + k_n\hat{x}_n(t) \\ & + w_n(t) + \hat{w}(t)\Big) \end{aligned} \tag{12}$$

where the control gains in (12) are calculated from

$$[\ k_1 \quad k_2 \quad \cdots \quad k_n\ ] = \mathcal{I}(\mathcal{T}_3 + h\mathcal{T}_4)^{-1}\mathcal{T}_2^\top$$

with $\mathcal{I} \triangleq [\ 1 \quad 0 \quad \cdots \quad 0\ ]$ and $h \triangleq R/(b_0^2Q)$.

For the purpose of practical implementation, estimates $\hat{x}_2(t), \cdots, \hat{x}_n(t)$ and $\hat{w}(t)$ should be generated by an observer. Before constructing the higher-order sliding mode observe, Assumption 1 has to be satisfied.

Assumption 1 ([28]). *There exist known constants $L \ge 0$ and $m \in \mathbb{N}_+$ such that $\left|w^{(m)}(t)\right| \le L$.*

As for motion control systems, the constant, slope and sine/cosine load torques are quite common in practice [35], and all of them are the special cases of Assumption 1. In this paper, a higher-order

sliding mode observe is designed as follows

$$\begin{aligned}\dot{\hat{x}}_i(t) &= \hat{x}_{i+1}(t) + v_i(t), i \in \mathbb{N}_{1:n-1}\\ \dot{\hat{x}}_n(t) &= -b_0 u^*(t) + w_n(t) + \hat{z}_1(t) + v_n(t)\\ \dot{\hat{z}}_j(t) &= \hat{z}_{j+1}(t) + v_{n+j}(t), j \in \mathbb{N}_{1:m-1}\\ \dot{\hat{z}}_m(t) &= v_{n+m}(t)\end{aligned} \tag{13}$$

where $v_1(t) \triangleq -\lambda_1 L^{\frac{1}{n+m}} |\hat{z}_1(t) - z_1(t)|^{\frac{n+m-1}{n+m}} \text{sign}\,(\hat{z}_1(t) - z_1(t))$, $v_k(t) \triangleq \lambda_k L^{\frac{1}{n+m+1-k}} |v_{k-1}(t)|^{\frac{n+m-k}{n+m+1-k}} \text{sign}\,(v_{k-1}(t))$, $k \in \mathbb{N}_{2:n+m}$ and $\lambda_l > 0$, $l \in \mathbb{N}_{1:n+m}$ are the tunable observer gains. The block diagram on the implementation of the proposed method is shown in Fig. 1.

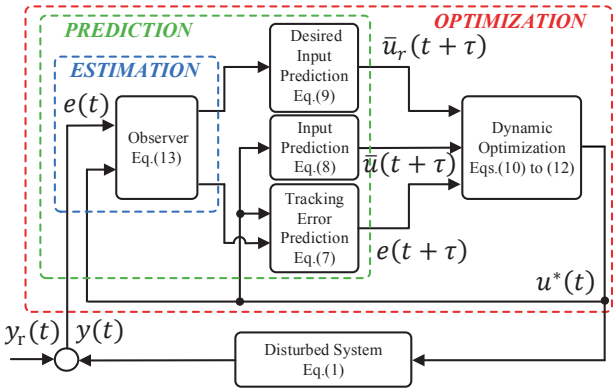

Fig. 1: Block diagram of the proposed method: Estimation, prediction and optimization

2.4 Performance Analysis

The main result on performance analysis is given by the following theorem.

Theorem 1. *Under Assumption 1, the closed-loop system (3)-(12)-(13) is asymptotically stable if and only if the control parameters of the proposed continuous-time MPC method are chosen such that the polynomial $p(s) = s^n + k_n s^{n-1} + \cdots + k_1$ is Hurwitz.*

Proof: See the Appendix A. □

In what follows, the direct relationship between the control parameters (the weighing matrices, Q and R, predictive period T and control order r) and the closed-loop system stability will be discussed. As a further result of [29], the concise description on stability conditions is shown in Table 1, which are discussed in details as the following three cases:

i) If system (1) has a low relative degree (1 or 2), the closed-loop system is always asymptotically stable no matter what parameters (Q, R, r and T) are chosen.
ii) If the relative degree of system (1) is 3 or 4, in the case when $R > 0$, the stability is ensured by assigning sufficiently large predictive period T; while in the case when $R = 0$, it will be always stable.
iii) If the relative degree of system (1) is higher ($n \geq 5$), the closed-loop system is unstable if r is too low; and if r has been properly chosen, the stability of the closed-loop system is the same as 2).

According to Theorem 1 and Table 1, the proposed method is able to achieve offset-free optimized tracking for the considered system

Table 1 Stability of the closed-loop system

n	1	2	3	4	5	6	7	8	9	10
$r=0$	$+^\star$	$+^\star$	$+$	$+$	$-$	$-$	$-$	$-$	$-$	$-$
$r=1$	$+^\star$	$+^\star$	$+$	$+$	$+$	$-$	$-$	$-$	$-$	$-$
$r=2$	$+^\star$	$+^\star$	$+$	$+$	$+$	$+$	$+$	$-$	$-$	$-$
$r=3$	$+^\star$	$+^\star$	$+$	$+$	$+$	$+$	$+$	$+$	$-$	$-$
$r=4$	$+^\star$	$+^\star$	$+$	$+$	$+$	$+$	$+$	$+$	$+$	$-$
$r=5$	$+^\star$	$+^\star$	$+$	$+$	$+$	$+$	$+$	$+$	$+$	$+$
$r=6$	$+^\star$	$+^\star$	$+$	$+$	$+$	$+$	$+$	$+$	$+$	$+$
$r=7$	$+^\star$	$+^\star$	$+$	$+$	$+$	$+$	$+$	$+$	$+$	$+$
$r=8$	$+^\star$	$+^\star$	$+$	$+$	$+$	$+$	$+$	$+$	$+$	$+$
$r=9$	$+^\star$	$+^\star$	$+$	$+$	$+$	$+$	$+$	$+$	$+$	$+$

$+^\star$: The closed-loop system is stable for any admissible control parameters.
$+$: If $R > 0$, the stability is ensured by assigning sufficiently large predictive period T; else if $R = 0$, the closed-loop system is always stable.
$-$: The closed-loop system is unstable.

with the presence of multiple kinds of disturbances and uncertainties by choosing appropriate parameters.

Remark 4 (Extension to Constraint Systems)**.** *The proposed MPC method can be extended for systems with input constraints by quadratic programming. For instance, the optimization problem (4) under the constraints $\mathcal{U}_{\min} \leq \mathcal{U} \leq \mathcal{U}_{\max}$ can be transformed as follows*

$$\begin{aligned}&\min\ \frac{1}{2} U^\top E U + U^\top F\\ &s.t.\ MU \leq \gamma\end{aligned} \tag{14}$$

where

$$U \triangleq \mathcal{U} - \frac{1}{b_0}(\mathcal{W}_n + \mathcal{W}),\ E \triangleq b_0^2 Q\mathcal{T}_3 + R\mathcal{T}_4$$
$$F \triangleq -b_0 Q\mathcal{T}_2^\top \bar{\mathcal{E}},\ M \triangleq [\mathcal{I}, -\mathcal{I}]^\top$$
$$\gamma \triangleq \left[\mathcal{U}_{\max} + \frac{1}{b_0}(\mathcal{W}_n + \mathcal{W}),\ -\mathcal{U}_{\min} - \frac{1}{b_0}(\mathcal{W}_n + \mathcal{W})\right]^\top$$

with $\mathcal{I}$ is an identity matrix. Notice that γ is associated with the original constraints on $\mathcal{U}$ and the values of $\mathcal{W}_n$ and $\mathcal{W}$. (14) is a standard quadratic programming problem and has been extensively studied in literature (see [12, Chapter 2.4, Numerical Solutions Using Quadratic Programming] for more details). With numerical solutions of quadratic programming, it is straightforward to deal with system constraints by the proposed method.

Remark 5 (Extension to Multivariable Systems)**.** *The proposed MPC method can be also extended for a class of multivariable nonlinear systems with well-defined relative degrees, even if they are different, i.e., $[\rho_1, \rho_2, \cdots, \rho_k]$ where $k \in \mathbb{N}_+$ is the number of the outputs/inputs. The basic idea is introduced in [36], i.e., to predict each output in receding-horizon by Taylor series expansion up to the orders $[r + \rho_1, r + \rho_2, \cdots, r + \rho_k]$.*

2.5 Numerical Simulation

A single-link robot arm system, as shown in Fig. 2, can be modeled as follows [37, Chapter 4.10]

$$\begin{aligned}J_1\ddot{q}_1 + F_1\dot{q}_1 + \frac{K}{N}(q_2 - \frac{q_1}{N}) &= u\\ J_2\ddot{q}_2 + F_2\dot{q}_2 + K(q_2 - \frac{q_1}{N}) + mgl\cos q_2 + d &= 0\end{aligned} \tag{15}$$

where u is the driving torque produced at the actuator axis; d is the disturbance torque at the link axis; q_1 and q_2 represent angular positions of the actuator shaft and of the link, respectively. The meanings and nominal values of robot arm parameters are listed in Table 2.

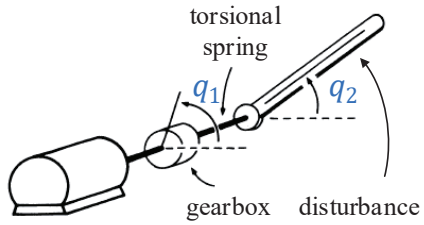

Fig. 2: A single-link robot arm

Table 2 Parameters of robot arm

Parameter	Meaning	Value	Unit
J_1	Inertia of actuator	0.0111	$\mathrm{kg \cdot m^2}$
F_1	Frictional coefficient of actuator	4.5	$\mathrm{N \cdot m \cdot s/rad}$
J_2	Inertia of link	0.2304185	$\mathrm{kg \cdot m^2}$
F_2	Frictional coefficient of link	0.084	$\mathrm{N \cdot m \cdot s/rad}$
K	Elasticity constant of spring	0.070364	$\mathrm{kg \cdot m^2}$
N	Transmission gear ratio	100	$\mathrm{N \cdot m \cdot s/rad}$
m	Mass of link	1	kg
g	Acceleration of gravity	9.8	$\mathrm{m/s^2}$
l	Position of link center	0.3493	m

In the simulation, the control objective is to render the link of the robot arm to asymptotically track the reference q_{2r} under the unknown external disturbance d. It is worth noting that the disturbance is mismatched from the control input channel and even its type is totally unknown. The control parameters are chosen as $q_{2r} = 0.5$(rad), $d = 0.5\sin(t)$(N·m), $n = 4$, $m = 2$, $[q_2(0), \dot{q}_2(0), q_1(0), \dot{q}_1(0); \hat{x}_1(0), \hat{x}_2(0), \hat{x}_3(0), \hat{x}_4(0); \hat{z}_1(0), \hat{z}_2(0)] = [0, 0, 0, 0; 0.5, 0, 0, 0; 0, 0]$, $h = 0$, $T = 0.02$, $r = 0$, $[\lambda_1, \lambda_2, \lambda_3, \lambda_4, \lambda_5, \lambda_6; L] = [25, 15, 10, 3, 1.5, 0.8; 800]$. Besides, a saturation from -500(N·m) to 500(N·m) is added on the control input for safety.

To make the simulation more challenging, parameter perturbations are artificially added in the robot arm system (15). The response curves of the angular positions of the actuator shaft and of the link, estimate of the lumped disturbance and driving torque are given in Fig. 3. To be more specific, the red dash lines and dot lines mean that all the system parameters have -30% and 30% uncertainties, respectively; the blue dash lines and dot lines mean that all the system parameters have -20% and 20% uncertainties, respectively; the green dash lines and dot lines mean that all the system parameters have -10% and 10% uncertainties, respectively; the black full lines means that the system parameters are the same with those in Table 2. Observed from the curves of the link q_2, one can arrive at that the asymptotic tacking can be achieved even under system uncertainties and external disturbances.

3 Application to a PMSM Servo System

In this section, experimental studies of a PMSM servo system are implemented to validate the feasibility and effectiveness of the proposed method. PMSMs are extensively applied to plenty of industrial applications, e.g., power generations, robotics, and aerospace [23, 27, 38]. Speed regulation of PMSM, regarded as a benchmark of the motion control problem here, is respectively solved by the proposed method and other effective MPC methods [12, 26]. One of the central control tasks of the motion control problem is to track the reference signal with satisfactory dynamic and steady-state performance, and to recover desired tracking performance even in the presence of large load torques.

Table 3 Parameters of PMSM servo system

Parameter	Meaning	Value	Unit
n_p	Number of poles-pairs	4	–
R	Stator resistance	9.7	Ω
L	Stator inductance	26	mH
ψ_f	Magnetic flux linkage	0.084	Wb
J	Moment of inertial	1.35×10^{-4}	$\mathrm{kg \cdot m^2}$
B_v	Frictional coefficient	7.4×10^{-5}	$\mathrm{N \cdot m \cdot s/rad}$

3.1 Dynamic Model Description

The dynamic model of a surface-mounted PMSM servo system is given in the rotor reference frame as [27]

$$\begin{aligned} \frac{di_d}{dt} &= \frac{1}{L}(u_d - Ri_d + n_p L\omega i_q) \\ \frac{di_q}{dt} &= \frac{1}{L}(u_q - Ri_q - n_p L\omega i_d - n_p\psi_f\omega) \\ \frac{d\omega}{dt} &= \frac{1}{J}\left(\frac{3}{2}n_p\psi_f i_q - B_v\omega - T_L\right) \end{aligned} \tag{16}$$

where ω is the rotor angular velocity; i_d and i_q are d- and q-axis stator currents, respectively; u_d and u_q are d- and q-axis stator voltages, respectively; and T_L is the load torque. The meanings and nominal values of PMSM parameters are listed in Table 3.

3.2 Design of Different MPC Methods

For speed regulation, system (16) is firstly rewritten as the considered standard one

$$\dot{x}_1 = x_2, \dot{x}_2 = -b_0 u_q + w_n + w \tag{17}$$

where

$$\begin{aligned} x_1 &\triangleq \omega_r - \omega,\ b_0 \triangleq 3n_p\psi_f/(2LJ),\ \varepsilon \triangleq -n_p\omega i_d \\ w_n &\triangleq \omega_r^{(2)} + (R/L + B_v/J)\omega_r^{(1)} \\ &\quad + \left(RB_v/(LJ) + 3n_p^2\psi_f^2/(2LJ)\right)\omega_r \\ &\quad - \left(RB_v/(LJ) + 3n_p^2\psi_f^2/(2LJ)\right)x_1 \\ &\quad - 3n_p\psi_f\varepsilon/(2J) \\ w &\triangleq RT_L/(LJ) + T_L^{(1)}/J - (R/L + B_v/J)x_2 \end{aligned}$$

ω_r is the reference speed. The control laws of the considered three MPC methods are presented as follows

i) The proposed method with performance index $J(t) = \frac{1}{2}\int_0^T \left(\|e(t+\tau)\|_Q^2 + \|u_r(t+\tau) - u_q(t+\tau)\|_R^2\right)d\tau$:

$$\text{Controller: } \left[u_q^* = \frac{1}{b_0}(k_1 x_1 + k_2\hat{x}_2 + w_n + \hat{w})\right.$$

$$\text{Observer: } \begin{cases} \dot{\hat{x}}_1 = \hat{x}_2 + v_1 \\ \dot{\hat{x}}_2 = -b_0 u_q^* + w_n + \hat{w} + v_2 \\ \dot{\hat{w}} = v_3 \\ v_1 = -\lambda_0 L^{\frac{1}{3}}|\hat{x}_1 - x_1|^{\frac{2}{3}}\mathrm{sign}(\hat{x}_1 - x_1) \\ v_i = \lambda_i L^{\frac{1}{4-i}}|v_{i-1}|^{\frac{3-i}{4-i}}\mathrm{sign}(v_{i-1}),\ i \in \mathbb{N}_{2:3} \end{cases}$$

where k_1 and k_2 are the optimized gains with zero control order, deduced as, $k_1 = 10T^2/(3T^4 + 60h)$ and $k_2 = 5T^3/(2T^4 + 40h)$.

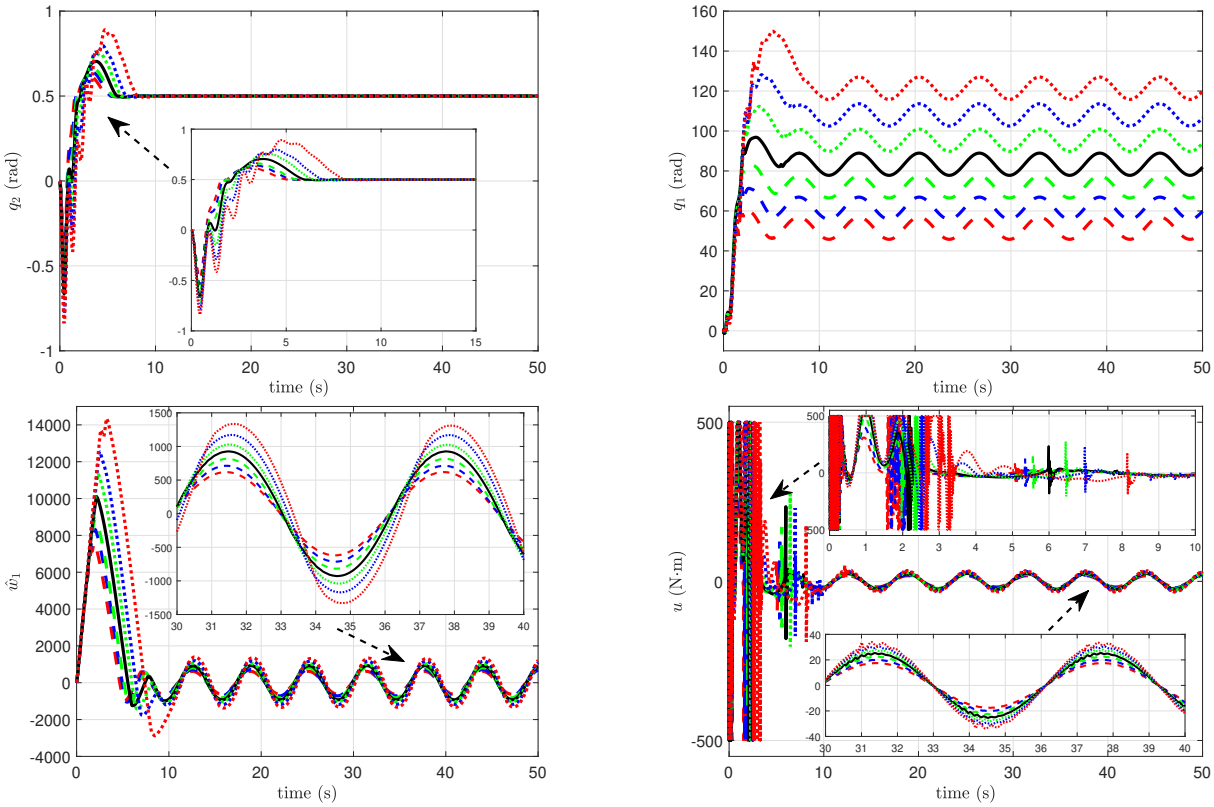

Fig. 3: System response of the robot arm under the proposed method

ii) The MPC method in [12] with performance index $J(t) = \frac{1}{2}\int_0^T \left(\|e(t+\tau)\|_Q^2 + \|\dot{u}_q(t+\tau)\|_R^2\right)d\tau$:

$$\text{Controller:} \begin{cases} u_q^* = \int_0^t \dot{u}_q^*(\tau)d\tau + u_q^*(0) \\ \dot{u}_q^* = \frac{1}{b_0}(k_1 x_1 + k_2\hat{x}_2 + k_3\hat{x}_3) \end{cases}$$

$$\text{Observer:} \begin{cases} \dot{\hat{x}}_1 = \hat{x}_2 + v_1 \\ \dot{\hat{x}}_2 = \hat{x}_3 + v_2 \\ \dot{\hat{x}}_3 = -b_0\dot{u}_q^* + v_3 \\ v_i(t) = -\lambda_i(\hat{x}_1 - x_1),\ i \in \mathbb{N}_{1:3} \end{cases}$$

where k_1, k_2 and k_3 are the optimized gains with zero control order, deduced as, $k_1 = 21T^3/(2T^6 + 504h)$, $k_2 = 42T^4/(5T^6 + 1260h)$ and $k_3 = 7T^5/(2T^6 + 504h)$.

iii) The MPC method in [26] with performance index $J(t) = \frac{1}{2}\int_0^T \left(\|e(t+\tau)\|_Q^2 + \|u_q(t+\tau)\|_R^2\right)d\tau$:

$$\text{Controller:} \begin{cases} u_q^* = \frac{1}{b_0}(k_1 x_1 + k_2\hat{x}_2 + k_w w_n + k_w\hat{w}) \end{cases}$$

$$\text{Observer:} \begin{cases} \dot{\hat{x}}_1 = \hat{x}_2 + v_1 \\ \dot{\hat{x}}_2 = -b_0 u_q^* + w_n + \hat{w} + v_2 \\ \dot{\hat{w}} = v_3 \\ v_i = -\lambda_i(\hat{x}_1 - x_1),\ i \in \mathbb{N}_{1:3} \end{cases}$$

where k_1, k_2 and k_w are the optimized gains with zero control order, deduced as, $k_1 = 10T^2/(3T^4 + 60h)$, $k_2 = 5T^3/(2T^4 + 40h)$ and $k_w = T^4/(T^4 + 20h)$.

Control parameters of these three approaches are chosen as $T = 0.002$, $R/Q = 0.0002$, $\lambda_1 = 4.1$, $\lambda_2 = 3.5$, $\lambda_3 = 2.0$ and $L = 7.2 \times 10^{11}$ for the proposed method; $T = 0.002$, $R/Q = 0.0005$, $\lambda_1 = 120$, $\lambda_2 = 1.5 \times 10^5$ and $\lambda_3 = 8 \times 10^6$ for the MPC method in [12]; and $T = 0.002$, $R/Q = 0.0002$, $\lambda_1 = 100$, $\lambda_2 = 6 \times 10^4$ and $\lambda_3 = 3 \times 10^6$ for the MPC method in [26].

Remark 6. *Note that the current i_d does not directly affect the speed ω and the control objective of d-axis current loop is relatively simple. Therefore, for the sake of simplicity, the conventional proportional-integral (PI) controller with decoupling is adopted as the d-axis controller, i.e.,*

$$u_d = k_p(-i_d) + k_i\int_0^t(-i_d)dt - n_p L\omega i_q$$

where k_p and k_i are the proportional and the integral gains, respectively. In the experiments, the proportional and integral gains of d-axis voltage of different MPC methods are all chosen as $k_p = 120$ and $k_i = 500$, respectively.

Remark 7. *Compared with the conventional MPC methods, the main deficiency is the difficulty in parameter tuning of the higher-order sliding mode disturbance observer. The parameter configuration for the higher-order sliding mode observer has certain restrictions, e.g., the fractional power should be strictly determined by the observer order. Besides, to the best of authors' knowledge, most published papers only focus on the stability, rather than the estimation performance of this kind of nonlinear observer. In the experimental application, trial and error approach based on the guideline in [39, Chapter 6.7, Arbitrary-Order Robust Exact Differentiation] has then been used to achieve desired performance.*

3.3 Experimental Results

To evaluate the performance of the proposed method, the experimental test setup is built as shown in Fig. 4. All the control algorithms

Table 4 Dynamic and steady-state tracking performance

Index	The proposed method	The MPC method in [12]	The MPC method in [26]
Settling time (ms)	46.6	62.4	56.5
Overshoot (%)	2.9	9.7	6.5
Offset error (rpm)	0.0	0.1	-25.7
Ripple range (rpm)	7.8	16.2	15.4

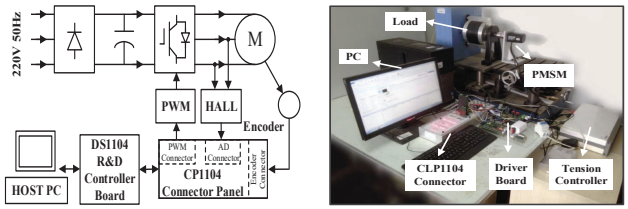

a *b*

Fig. 4: Experimental system
a Configuration
b Setup

are done by dSPACE DS1104 control board, which is a completely real-time control system based on a 603 Power PC floating-point processor running at 250 MHz and includes a four-channel 16-bit (multiplexed) ADC and four 12-bit ADC units. The power driving circuit is composed of IGBT inverter, single-phase of diode bridge rectifier, and large capacitor filter, etc. Both the control and sample periods are 100 μs. The dead time and the switching frequency of IGBTs is 3 μs and 10 kHz. The signals of voltages and currents can be measured by Hall sensors whilst the position is obtained by an incremental encoder with 2500 lines. The speed single is calculated from low pass filter of position differential.

3.3.1 Dynamic/Steady-State Tracking Performance Tests: In this subsection, dynamic performance and tracking precision in steady states of a PMSM servo system under the proposed method, the MPC methods in [12] and [26] are thoroughly compared and studied. Response curves of speed ω and voltage u_q under all the three methods are demonstrated in Figs. 5 and 6.

Case I–Dynamic Tracking performance.

As shown by Fig. 5, the PMSM under the proposed method presents a shortest settling time (46.6ms) and a smallest overshoot (2.9%) during the transient dynamics, and no offset error in the steady state. Even the PMSM under the MPC method in [26] has similar performance in the dynamic phase, it cannot track the reference offset-free. The reason for this phenomenon can be found in its eventual expression of controller, i.e., the compensation gain k_w of the MPC in [26] is always less than 1, which results in the offset error between the control input and the desired one in the steady state and is finally reflected in the speed tracking. In addition, although offset-free property is guaranteed by the MPC in [12], its dynamic performanceperformance is the worst, e.g., the longest settling time (62.4ms) and the largest overshoot (9.7%).

Case II–Steady-State Tracking performance.

As shown by Fig. 6, there exist steady-state fluctuations for all the three controllers, while the proposed method shows the smallest fluctuations (7.8rpm) in the steady state. It is observed from Fig. 5 (d) that fluctuations of the PMSM with the proposed method are reduced by 50.1% and 48.1% compared to the MPC methods in [12] and [26], respectively. Detailed quantitative data for dynamic and steady-state performance comparisons of Cases I and II are given in Table 4.

3.3.2 Disturbance Rejection Performance Tests: This case is designed to verify the robustness of the three controllers against external load disturbances. Both constant and time-varying loads are

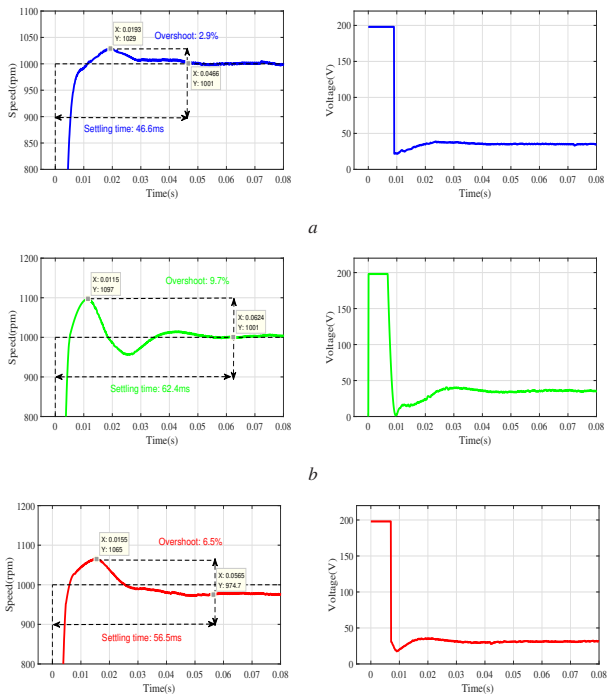

a
b
c

Fig. 5: Case I–Dynamic tracking performance of the PMSM servo system
a The proposed method
b The MPC method in [12]
c The MPC method in [26]

imposed on the motor as follows

$$T_L(\mathrm{N}\cdot\mathrm{m}) = \begin{cases} 0 & 0\mathrm{s} \le t < 0.5\mathrm{s} \\ 1 & 0.5\mathrm{s} \le t < 1\mathrm{s} \\ 1 + 0.5\sin(50\pi t + \pi/3) & t \ge 1\mathrm{s}. \end{cases}$$

Case III–Constant Load Torque Rejection.

Response curves of the speed ω and the voltage u_q when a step load (from 0N · m to 1N · m at 0.5s) is imposed on the motor under all the three methods are demonstrated in Fig. 7. It is revealed that performance of the proposed method is much better than the other two in the sense that it has the shortest recovery time (85.6ms), the smallest speed drop (43.5rpm), and presents offset-free tracking behavior. Similar with Case II, the robust MPC method in [26] cannot completely compensate the effect of constant load, and then, the speed cannot recover to its desired reference, as shown in the red line of Fig. 7.

Case IV–Time-Varying Load Torque Rejection.

To further compare disturbance rejection performanceperformance, periodic load torque is considered in this case. As shown in Fig. 8, the tracking precision is substantially improved by the proposed method. Compared to the MPC methods in [12] and [26], the fluctuations of the proposed method are reduced by 74.4% and

Table 5 Load torque rejection performance

Index	The proposed method	The MPC method in [12]	The MPC method in [26]
Recovery time (ms)	85.6	123.2	106.5
Maximum speed drop (rpm)	43.5	129.2	99.8
Offset error (rpm)	0.3	-0.7	-85.5
Ripple range (rpm)	25.7	98.8	62.0

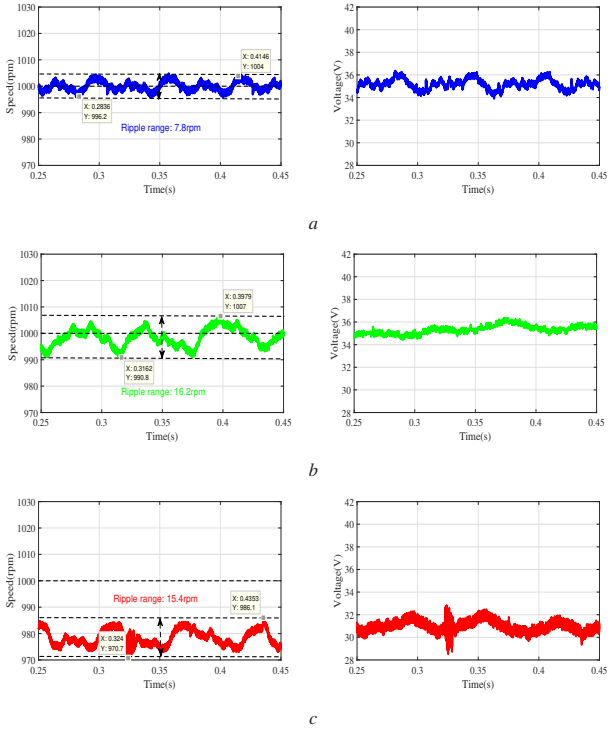

Fig. 6: Case II–Steady-state tracking performance of the PMSM servo system
a The proposed method
b The MPC method in [12]
c The MPC method in [26]

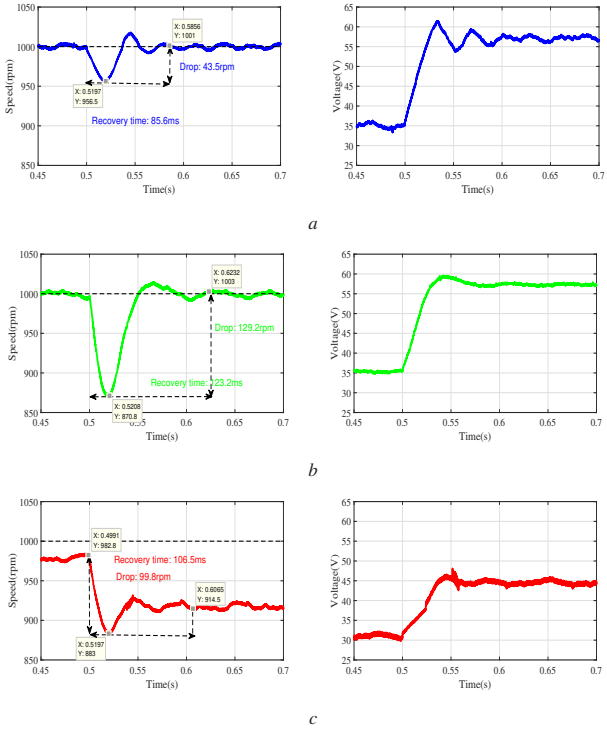

Fig. 7: Case III–Constant load torque rejection of the PMSM servo system
a The proposed method
b The MPC method in [12]
c The MPC method in [26]

59.0%, respectively. More detailed quantitative performance index comparisons of Cases III and IV are provided in Table 5.

On the basis of the above experimental results and analyses, it is concluded that the proposed method possesses a better dynamic performance and a higher tracking precision, even in the presence of multiple kinds of disturbances and uncertainties.

4 Conclusion

A nonlinear-disturbance-observer-enhanced continuous-time MPC approach has been proposed to achieve optimized offset-free tracking for motion control systems with multiple kinds of disturbances in this paper. A new performance index that integrating the desired steady-state control input has been proposed, which leads to the offset-free tracking property and provides additional freedom on penalizing the control input. The stability of the closed-loop system has been rigorously developed. A PMSM servo system has been conducted to illustrate the feasibility and efficacy of the proposed method. It has been shown that the proposed control approach exhibits remarkable tracking and anti-disturbance performances as compared with other two robust MPC methods.

5 Acknowledgments

This work was supported in part by the National Natural Science Foundation of China under Grant Nos. 61903186, 61973080, 61973081 and 61750110525, in part by the Natural Science Foundation of Jiangsu Province, China under Grant No. BK20190665, in part by FRC Tier 1 grant with WBS No. R397-000-302-114 from faculty of engineering, National University of Singapore, in part by the State Scholarship Fund under Grant No. 201706090111.

6 Appendices

The following lemma plays an important role in the proof of Theorem 1.

Lemma 1 (Schur Decomposition Bound, [40]). *The inequality* $\|\exp(At)\| \leq \exp(\alpha(A)t) \sum_{k=0}^{n-1} \|Nt\|^2/k!$ *holds for* $A \in \mathbb{R}_{n\times n}$, *where* $\alpha(A) \in \mathbb{R}$ *is the maximum real part of eigenvalues of* A *and* $N \in \mathbb{R}_{n\times n}$ *is the Schur decomposition matrix of* A.

Proof: It is divided into two steps. The first step is to prove that the estimates in the observer (13) will respectively converge to their

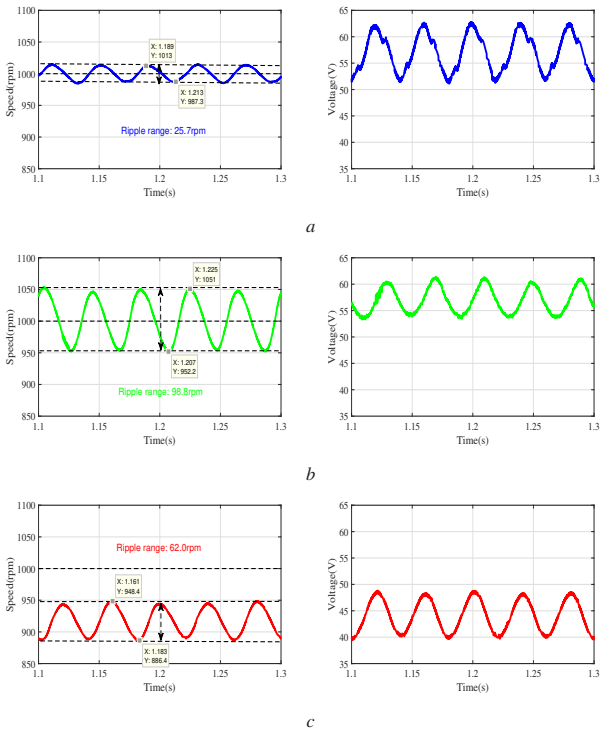

Fig. 8: Case IV–Time-varying load torque rejection of the PMSM servo system
a The proposed method
b The MPC method in [12]
c The MPC method in [26]

truth-values within finite time. The second step is to prove that the closed-loop system (3)-(12)-(13) is asymptotically stable.

1) First Step:

Let the estimation errors as $\sigma_i \triangleq \hat{x}_i(t) - x_i(t)$, $i \in \mathbb{N}_{1:n}$ and $\sigma_{n+j} \triangleq \hat{z}_j(t) - z_j(t)$, $j \in \mathbb{N}_{1:m}$. The error dynamics is then governed by

$$\begin{aligned}
\dot{\sigma}_1 &= -\lambda_1 L^{\frac{1}{n+m}} |\sigma_1|^{\frac{n+m-1}{n+m}} \operatorname{sign}(\sigma_1) + \sigma_2 \\
\dot{\sigma}_i &= -\lambda_i L^{\frac{1}{n+m+1-i}} |\sigma_i - \dot{\sigma}_{i-1}|^{\frac{n+m-i}{n+m+1-i}} \operatorname{sign}(\sigma_i - \dot{\sigma}_{i-1}) \\
&\quad + \sigma_{i+1}, i \in \mathbb{N}_{2:n+m-1} \\
\dot{\sigma}_{n+m} &\in -\lambda_{n+m} L \operatorname{sign}(\sigma_{n+m} - \dot{\sigma}_{n+m-1}) + [-L, L].
\end{aligned} \tag{18}$$

It follows from [28] that the estimation error system (18) is finite time stable, i.e., there exists a finite time instant $0 < t_f < \infty$ such that $\sigma_j(t)$, $j \in \mathbb{N}_{1:n+m}$ are bounded if $0 \le t < t_f$ and $\sigma_j(t) \equiv 0$ else if $t \ge t_f$.

2) Second Step:

With the observer error dynamics (18) in mind, inserting the MPC law (12) into the output tracking error system (3) gives

$$e^{(n)}(t) + k_n e^{(n-1)}(t) + \cdots + k_1 e(t) + g(t) = 0 \tag{19}$$

where $g(t) \triangleq k_2\sigma_2 + \cdots + k_n\sigma_n + \sigma_{n+1}$. Since k_i, $i \in \mathbb{N}_{1:n}$ are bounded, it follows from the result in *First Step* that $g(t)$ is bounded for $0 \le t < t_f$ and $g(t) \equiv 0$ for $t \ge t_f$. Rewrite system (19) in the following compact form

$$\dot{\mathcal{E}}(t) = \mathcal{A}\mathcal{E}(t) + \mathcal{B}g(t) \tag{20}$$

where

$$\begin{aligned}
\mathcal{E} &\triangleq [\ x_1(t) \quad x_2(t) \quad \cdots \quad x_n(t)\ ]^\top \\
\mathcal{A} &\triangleq \begin{bmatrix} \mathcal{O} & \mathcal{I} \\ -k_1 & \beta \end{bmatrix} \\
\beta &\triangleq [\ -k_2 \quad -k_3 \quad \cdots \quad -k_n\ ] \\
\mathcal{B} &\triangleq [\ 0 \quad 0 \quad \cdots \quad -1\ ]^\top
\end{aligned}$$

with $\mathcal{I}$ and $\mathcal{O}$ are identity matrix and zero matrix.

The solution $\mathcal{E}(t)$ of (20) is represented as $\mathcal{E}(t) = \exp(\mathcal{A}t)\mathcal{E}(0) + \int_0^t \exp(\mathcal{A}(t-\tau))\mathcal{B}g(\tau)d\tau$. It follows from the above equality that $\|\mathcal{E}(t)\| \le \|\exp(\mathcal{A}t)\mathcal{E}(0)\| + \int_0^t \|\exp(\mathcal{A}(t-\tau))\| \cdot |g(\tau)|d\tau$. Letting the upper bound of $|g(t)|$ as $\gamma \ge 0$, i.e., $\forall t \ge 0$, $|g(t)| \le \gamma$, one have the following inequality

$$\|\mathcal{E}(t)\| \le \|\exp(\mathcal{A}t)\| \cdot \|\mathcal{E}(0)\| + \gamma \int_0^t \|\exp(\mathcal{A}\tau)\| d\tau.$$

With the help of Lemma 1, in the case when $\alpha(\mathcal{A}) \neq 0$, one arrives at that

$$\begin{aligned}
\|\mathcal{E}(t)\| &\le \delta t^2 \exp(\alpha(\mathcal{A})t) \|\mathcal{E}(0)\| \\
&\quad + \frac{\delta\gamma}{\alpha(\mathcal{A})^3} \left(\left(\alpha(\mathcal{A})^2 t^2 - 2\alpha(\mathcal{A})t + 2 \right) \exp(\alpha(\mathcal{A})t) - 2 \right)
\end{aligned}$$

and in the case when $\alpha(\mathcal{A}) = 0$, one arrives at that

$$\|\mathcal{E}(t)\| \le \delta t^2 \|\mathcal{E}(0)\| + \frac{\delta\gamma}{3} t^3$$

where $\delta \triangleq \sum_{k=0}^{n-1} \|\mathcal{N}\|^2/k! \ge 0$ and $\mathcal{N}$ is the Schur decomposition matrix of $\mathcal{A}$.

Since the upper-bound function of $\|\mathcal{E}(t)\|$ is elementary without any singular point, it can be concluded that within any finite time interval (e.g., $0 \le t < t_f$), $\|\mathcal{E}(t)\|$ is bounded whether $\mathcal{A}$ is Hurwitz or not. Furthermore, if $t \ge t_f$, system (20) is reduced to $\dot{\mathcal{E}}(t) = \mathcal{A}\mathcal{E}(t)$. Note that the characteristic polynomial of $\mathcal{A}$ is deduced as $p(s) = s^n + k_n s^{n-1} + \cdots + k_1$. Therefore, the sufficient and necessary condition of asymptotic stability is that $p(s)$ is Hurwitz. This completes the proof. □

7 References

1 Richalet, J.: 'Industrial applications of model based predictive control', *Automatica*, 1993, **29**, (5), pp. 1251–1274
2 Morari, M., Lee, J.H.: 'Model predictive control: Past, present and future', *Computers & Chemical Engineering*, 1999, **23**, (4-5), pp. 667–682
3 Mayne, D.Q., Rawlings, J.B., Rao, C.V., Scokaert, P.O.: 'Constrained model predictive control: Stability and optimality', *Automatica*, 2000, **36**, (6), pp. 789–814
4 Pourkargar, D.B., Almansoori, A., Daoutidis, P.: 'Impact of decomposition on distributed model predictive control: A process network case study', *Industrial & Engineering Chemistry Research*, 2017, **56**, (34), pp. 9606–9616
5 Pourkargar, D.B., Almansoori, A., Daoutidis, P.: 'Comprehensive study of decomposition effects on distributed output tracking of an integrated process over a wide operating range', *Chemical Engineering Research and Design*, 2018, **134**, pp. 553–563
6 Tang, W., Pourkargar, D.B., Daoutidis, P.: 'Relative time-averaged gain array (RTAGA) for distributed control-oriented network decomposition', *AIChE Journal*, 2018, **64**, (5), pp. 1682–1690
7 Kong, L., Yuan, J.: 'Disturbance-observer-based fuzzy model predictive control for nonlinear processes with disturbances and input constraints', *ISA transactions*, 2019, published online
8 Hermansson, A.W., Syafiie, S.: 'An offset-free MPC formulation for nonlinear systems using adaptive integral controller', *ISA transactions*, 2019, published online
9 Muske, K.R., Badgwell, T.A.: 'Disturbance modeling for offset-free linear model predictive control', *Journal of Process Control*, 2002, **12**, (5), pp. 617–632
10 Maeder, U., Borrelli, F., Morari, M.: 'Linear offset-free model predictive control', *Automatica*, 2009, **45**, (10), pp. 2214–2222
11 Morari, M., Maeder, U.: 'Nonlinear offset-free model predictive control', *Automatica*, 2012, **48**, (9), pp. 2059–2067

12 Wang, L.: 'Model predictive control system design and implementation using MATLAB®'. (Springer Science & Business Media, 2009)
13 Zhao, H., Ren, B., Chen, H., Deng, W.: 'Model predictive control allocation for stability improvement of four-wheel drive electric vehicles in critical driving condition', *IET Control Theory & Applications*, 2015, **9**, (18), pp. 2688–2696
14 Alexis, K., Nikolakopoulos, G., Tzes, A.: 'Model predictive quadrotor control: attitude, altitude and position experimental studies', *IET Control Theory & Applications*, 2012, **6**, (12), pp. 1812–1827
15 Yang, H., Guo, M., Xia, Y., Cheng, L.: 'Trajectory tracking for wheeled mobile robots via model predictive control with softening constraints', *IET Control Theory & Applications*, 2017, **12**, (2), pp. 206–214
16 Ang, K.H., Chong, G., Li, Y.: 'PID control system analysis, design, and technology', *IEEE transactions on control systems technology*, 2005, **13**, (4), pp. 559–576
17 Ohnishi, K., Shibata, M., Murakami, T.: 'Motion control for advanced mechatronics', *IEEE/ASME Transactions On Mechatronics*, 1996, **1**, (1), pp. 56–67
18 Han, J.: 'From PID to active disturbance rejection control', *IEEE transactions on Industrial Electronics*, 2009, **56**, (3), pp. 900–906
19 Chen, W.H., Yang, J., Guo, L., Li, S.: 'Disturbance-observer-based control and related methods—An overview', *IEEE Transactions on Industrial Electronics*, 2016, **63**, (2), pp. 1083–1095
20 Yan, Y., Zhang, C., Liu, C., Yang, J., Li, S.: 'Disturbance rejection for nonlinear uncertain systems with output measurement errors: Application to a helicopter model', *IEEE Transactions on Industrial Informatics*, 2019, published online
21 Liu, C., Chen, W.H., Andrews, J.: 'Tracking control of small-scale helicopters using explicit nonlinear MPC augmented with disturbance observers', *Control Engineering Practice*, 2012, **20**, (3), pp. 258–268
22 Xia, C., Wang, M., Song, Z., Liu, T.: 'Robust model predictive current control of three-phase voltage source PWM rectifier with online disturbance observation', *IEEE Transactions on Industrial Informatics*, 2012, **8**, (3), pp. 459–471
23 Errouissi, R., Ouhrouche, M., Chen, W.H., Trzynadlowski, A.M.: 'Robust nonlinear predictive controller for permanent-magnet synchronous motors with an optimized cost function', *IEEE Transactions on Industrial Electronics*, 2012, **59**, (7), pp. 2849–2858
24 Pannocchia, G., Bemporad, A.: 'Combined design of disturbance model and observer for offset-free model predictive control', *IEEE Transactions on Automatic Control*, 2007, **52**, (6), pp. 1048–1053
25 Chen, W.H., Ballance, D.J., Gawthrop, P.J., Gribble, J.J., O'Reilly, J.: 'Nonlinear PID predictive controller', *IEE Proceedings-Control Theory and Applications*, 1999, **146**, (6), pp. 603–611
26 Yang, J., Zheng, W.X., Li, S., Wu, B., Cheng, M.: 'Design of a prediction-accuracy-enhanced continuous-time MPC for disturbed systems via a disturbance observer', *IEEE Transactions on Industrial Electronics*, 2015, **62**, (9), pp. 5807–5816
27 Yan, Y., Yang, J., Sun, Z., Zhang, C., Li, S., Yu, H.: 'Robust speed regulation for PMSM servo system with multiple sources of disturbances via an augmented disturbance observer', *IEEE/ASME Transactions on Mechatronics*, 2018, **23**, (2), pp. 769–780
28 Levant, A.: 'Higher-order sliding modes, differentiation and output-feedback control', *International Journal of Control*, 2003, **76**, (9-10), pp. 924–941
29 Chen, W.H., Ballance, D.J., Gawthrop, P.J.: 'Optimal control of nonlinear systems: A predictive control approach', *Automatica*, 2003, **39**, (4), pp. 633–641
30 Yu, H., Huang, S., Chen, G., Pan, Y., Guo, Z.: 'Human–robot interaction control of rehabilitation robots with series elastic actuators', *IEEE Transactions on Robotics*, 2015, **31**, (5), pp. 1089–1100
31 Sariyildiz, E., Sekiguchi, H., Nozaki, T., Ugurlu, B., Ohnishi, K.: 'A stability analysis for the acceleration-based robust position control of robot manipulators via disturbance observer', *IEEE/ASME Transactions on Mechatronics*, 2018,
32 Sariyildiz, E., Chen, G., Yu, H.: 'A unified robust motion controller design for series elastic actuators', *IEEE/ASME Transactions on Mechatronics*, 2017, **22**, (5), pp. 2229–2240
33 Siller.Alcalá, I.I. 'Nonlinear continuous-time generalised predictive control'. University of Glasgow, 1998
34 Yan, Y., Zhang, C., Narayan, A., Yang, J., Li, S., Yu, H.: 'Generalized dynamic predictive control for nonparametric uncertain systems with application to series elastic actuators', *IEEE Transactions on Industrial Informatics*, 2018, **14**, (11), pp. 4829–4840
35 Yang, J., Chen, W.H., Li, S., Guo, L., Yan, Y.: 'Disturbance/uncertainty estimation and attenuation techniques in PMSM drives—A survey', *IEEE Transactions on Industrial Electronics*, 2016, **64**, (4), pp. 3273–3285
36 Chen, W.H. 'Closed-form nonlinear MPC for multivariable nonlinear systems with different relative degree'. In: Proceedings of the American Control Conference. (, 2003. pp. 4887–4892
37 Isidori, A.: 'Nonlinear control systems'. (Springer Science & Business Media, 2013)
38 Niu, X., Zhang, C., Li, H.: 'Active disturbance attenuation control for permanent magnet synchronous motor via feedback domination and disturbance observer', *IET Control Theory & Applications*, 2017, **11**, (6), pp. 807–815
39 Shtessel, Y., Edwards, C., Fridman, L., Levant, A.: 'Sliding mode control and observation'. (Springer, 2014)
40 Van.Loan, C.: 'The sensitivity of the matrix exponential', *SIAM Journal on Numerical Analysis*, 1977, **14**, (6), pp. 971–981